CRACK PROPAGATION IN MIXED MODE FRACTURE OF CONCRETE

P.C. Olsen[1]

[1]Man., Tech. Dir. Colberg Consult, Fasanvænget 124, 2980 Kokkedal, Denmark.

ABSTRACT

The paper is concerned with the application of the Hillerborg fictitious crack model in mixed mode I-II fracture of concrete. It is shown that the cohesive normal traction between opposite crack faces removes all stress singularities at the crack tip, provided that the direction of the crack propagation follows a path of minimum potential energy. In addition, the stresses at the crack tip are hydrostatic. Therefore, these stresses do not reveal a preferable direction of crack propagation. Also, as stresses are finite, stress intensity factors are all zero and K_I-K_{II} concepts cannot reveal a direction of propagation. A new concept of determining the direction of crack propagation based on a "predictor-corrector" principle is presented, in which, firstly, the crack is advanced tangentially into the uncracked concrete, the predictor. Thereafter the direction is updated using a corrector. Based on the J, L and M integrals of the conservation laws, two proposals for the updated direction are presented.

KEYWORDS

Non-linear fracture mechanics, fictitious crack model, mixed mode fracture, crack propagation, conservation laws, boundary element method.

INTRODUCTION

The original concept of the fictitious crack model proposed by Hillerborg [1] relies on the existence of a σ-δ relationship, i.e. a relationship between normal stresses and crack opening width, and that a crack propagates when the stress at the crack tip exceeds the tensile strength. Mixed mode fracture was not originally considered. However, Peterson [2], although investigating mode-I fracture only, implied that the fictitious crack model is valid also for mixed mode fracture, and proposed that the crack would propagate in a direction perpendicular to the first principal stress. Ingraffea and Samoua [3] applied the fictitious crack model using the FEM-method in mixed mode fracture, determining the direction of crack propagation based on K_I-K_{II} concepts.

However, by observing stresses and corresponding external loads, the author found in his research that the cohesive normal traction between opposite crack faces removes all stress singularities at the crack tip, provided that the direction of the crack propagation follows a path of minimum potential energy. In addition, the stresses at the crack tip are hydrostatic. Therefore these stresses do not reveal a preferable direction of crack propagation. Also, as stresses are finite, stress intensity factors are all zero and K_I-K_{II} concepts cannot

reveal a direction of propagation either. The direction of crack propagation determined by one of the principles above will therefore be coincidental, the paradox arising, that one gets an answer for an "incorrect" current crack tip position only, at which stresses are infinite and not hydrostatic.

The energy release rates for various changes in defects can be determined by evaluation of the *J, L* and *M* integrals as shown by Eshelby [4] and Budiansky/Rice [5]. Applying their results, the author presents two proposals for determining the direction of crack propagation based on a direction of maximum change in energy release rate, as determined by the *J, L* and *M* integrals. All results presented are based on the application of the boundary element method (BEM).

THE BEM-METHOD AS VEHICLE FOR THE FICTITIOUS CRACK MODEL

The basic equation in the boundary element method is the extended Somigliano's identity, valid for both internal points and for points on the boundary:

$$C_{ij}(s)u_j(s) + \int_{\Gamma} \overline{p}_{ij}(s,q)u_j(q)d\Gamma = \int_{\Gamma} \overline{u}_{ij}(s,q)p_j(s)d\Gamma + \int_{\Omega} \overline{u}_{ij}(s,q)b_j(q)d\Omega \qquad (1)$$

where $u_{ij}(s,q)$ and $p_{ij}(s,q)$ are the fundamental solutions for displacements and tractions respectively for a unit point load. $u_j(q)$ and $p_j(q)$ are the displacements and tractions respectively at the boundary. $b_j(q)$ is the body force, $C_{ij}(s)$ is a matrix depending upon the boundary shape, Ω is the domain considered and Γ the corresponding boundary. The reader is referred to literature for the fundamentals of the boundary element method, for example Brebbia et al [6]. Applying the multi-domain BEM-method, the fracture process zone could be embedded directly in the boundary element method by means of non-linear interface conditions, depicted by matrix *S* in Fig. 1. However, the principle of superposition as devised by Peterson [2] for mode-I fracture is more appropriate for the objectives in this paper. In this method the boundary element method merely serves as a device to determine influence coefficients.
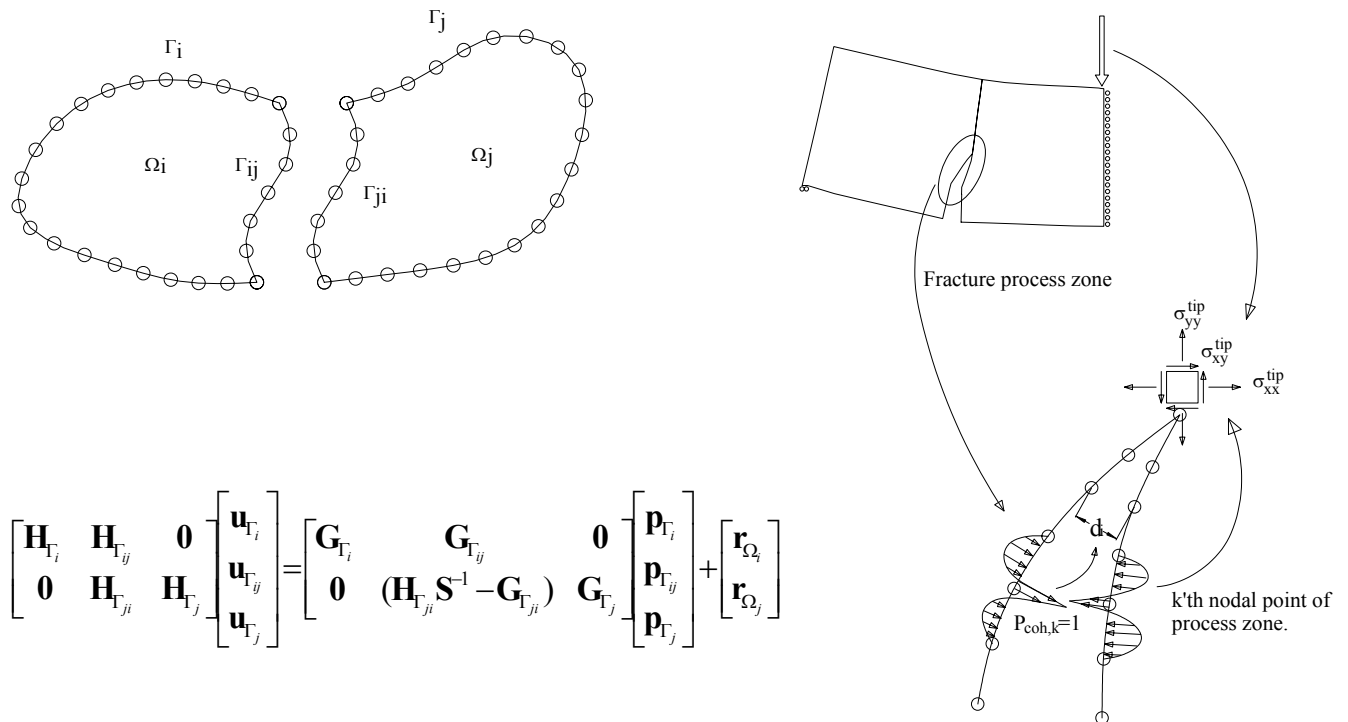

$$\begin{bmatrix} \mathbf{H}_{\Gamma_i} & \mathbf{H}_{\Gamma_{ij}} & \mathbf{0} \\ \mathbf{0} & \mathbf{H}_{\Gamma_{ji}} & \mathbf{H}_{\Gamma_j} \end{bmatrix} \begin{bmatrix} \mathbf{u}_{\Gamma_i} \\ \mathbf{u}_{\Gamma_{ij}} \\ \mathbf{u}_{\Gamma_j} \end{bmatrix} = \begin{bmatrix} \mathbf{G}_{\Gamma_i} & \mathbf{G}_{\Gamma_{ij}} & \mathbf{0} \\ \mathbf{0} & (\mathbf{H}_{\Gamma_{ji}}\mathbf{S}^{-1} - \mathbf{G}_{\Gamma_{ji}}) & \mathbf{G}_{\Gamma_j} \end{bmatrix} \begin{bmatrix} \mathbf{p}_{\Gamma_i} \\ \mathbf{p}_{\Gamma_{ij}} \\ \mathbf{p}_{\Gamma_j} \end{bmatrix} + \begin{bmatrix} \mathbf{r}_{\Omega_i} \\ \mathbf{r}_{\Omega_j} \end{bmatrix}$$

Figure 1 The multi-domain BEM-method for the fictitious crack model.

The objective is, for a given crack tip position, not necessarily the correct one, to determine an external load that complies with the following conditions: 1) the first principal stress in front of the crack tip equals the tensile strength and 2) normal stresses and crack widths in the crack process zone comply with the $\sigma-\delta$ relationship.
The external load naturally causes deformations and the crack to widen. On the other hand, the traction in the fracture process zone attempts to attract the two crack surfaces to each other. To determine the external

load, the stresses at the crack tip and the crack width along the crack surface are firstly determined for a unit external load. Secondly, for unit normal tractions at all the nodes along the crack surface, the stresses at the crack tip and the crack width along the crack surface are determined (see Fig. (1)). The total stress σ_{ij}^{tip} at the crack tip is thus composed of a linear combination of the stress from the external load and stresses from the cohesive tractions as follows:

$$\sigma_{ij}^{tip} = \lambda \sum_{k=1}^{n} \sigma_{ij,k}^{tip} p_{coh,k} + \sigma_{ij,p}^{tip} \tag{2}$$

where index p indicates the stresses from the unit external load and index k the stresses from the individual unit cohesive tractions along the process zone. Similarly, the crack width at the nodal points along the crack surface δ_i are composed of a linear combination of crack width from the external load and crack width from the cohesive tractions along the crack surface:

$$\delta_i = \lambda \sum_{k=1}^{n} \delta_{ik} p_{coh,k} + \delta_{i,p} \tag{3}$$

where $\delta_{i,p}$ are the crack width from the unit external load and δ_{ik} the crack width from the individual unit cohesive tractions along the process zone.

Having determined the influence coefficients above, the external load and the crack width profile that comply with the objectives above, can now be determined. This can only be accomplished iteratively. To assure convergence, a displacement-controlled procedure must be used. The crack opening opposite the crack tip, say δ_n, is used as control parameter. For a given value of the control parameter $\bar{\delta}_n$, the cohesive tractions $p_{coh,i}$ are firstly initialised, for example setting $p_{coh,i}=f_t$. With this initial guess, a load factor is determined from Eqn. 4:

$$\lambda = (\bar{\delta}_n - \sum_{i=1}^{n} \delta_{n,i} \times p_{coh,i}) / \delta_{n,p} \tag{4}$$

The crack openings δ_i at the other nodal points can now be determined and from the $\sigma - \delta$ relationship the cohesive tractions at the nodal points are updated. A new load factor is computed and so forth until the cohesive tractions stabilise. From Eqn. 5 the stress tensor at the crack tip is hereafter evaluated and the first principal stress is determined:

$$\sigma_1 = 0.5(\sigma_{xx}^{tip} + \sigma_{yy}^{tip} + \sqrt{(\sigma_{xx}^{tip} - \sigma_{yy}^{tip})^2 + 4\sigma_{xy}^{tip\,2}}) \tag{5}$$

The value of the control parameter is hereafter iteratively altered, for example using the bi-section method, until the requirement $\sigma_1=f_t$ is satisfied.

OBSERVING VARIOUS CRACK TIP POSITIONS

A three point bending beam with a flat notch placed in the shear zone is now considered. The depth of the beam is $d=400mm$, the width $b=1000mm$ and the length $l=1600mm$. The notch has a depth of $d'=100mm$ and is situated a distance $a=400mm$ from the centre line of the beam. The size of the support areas are $l_s=16mm$, whereas the point load at the centre of the beam is distributed over an area of $l_p=32mm$. Due to symmetry only half of the beam is modelled. A straight crack originating at the root of the notch, having a length of $h=100mm$ is considered. The concrete tensile strength is $f_t=4MPa$, the modulus of elasticity $E=40GPa$ and the fracture energy $G=100N/m$, the $\sigma - \delta$ relationship varying linearly.

Applying the principles described in the previous section, the stress distribution in front of the crack has been observed for various positions of the crack tip, expressed by means of the angle v, by which the crack direction deviates from vertical. In Fig. (2) the normal traction, the tangential traction and the tangential normal stress, all with respect to the sub-domain boundaries, are plotted for crack tip positions corresponding to $v=15°$, $v=20°$ and $v=25°$. It is easily recognized that for $v=15°$ and for $v=25°$ the tangential traction tends towards infinity, however, with opposite sign for the two crack tip positions. At $v=20°$, the tangential traction at the crack tip almost equals zero. The normal traction and the tangential normal stress

are almost continuous across the crack tip and it can be concluded that stress singularities are not present for this particular position of the crack tip.
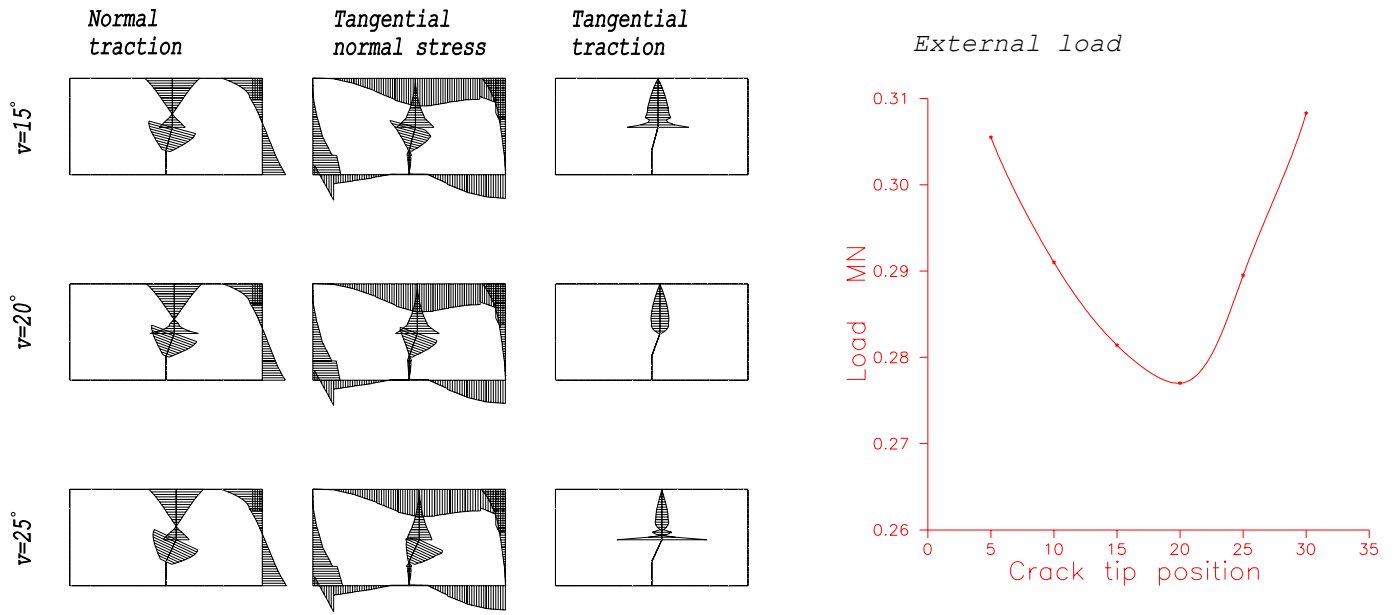

Figure 2 Observing external load and associated stresses for various crack tip positions.

In Fig. (2) the external load is plotted for the various crack tip positions as well. It is observed that the external load is minimal for $v=20^o$, i.e. for the crack tip position at which the stress singularities are all removed. The important observation is made that, following a crack path other than the one corresponding to continuous smoothness of stresses at the crack tip, one does not follow a path of minimum potential energy configuration.

DEFECT VARIATIONS AND RELATED ENERGY RELEASE RATES

The conservation laws are the direct consequence of the basic equations of the theory of elasticity. Knowles and Sternberg [7] have shown that, when these equations are all satisfied, the following integrals:

$$J_x = \int_S (Wn_x - (p_x \varepsilon_{xx} + p_y \frac{\partial u_y}{\partial x}))dS \tag{6}$$

$$J_y = \int_S (Wn_y - (p_x \frac{\partial u_y}{\partial x} + p_y \varepsilon_{yy}))dS \tag{7}$$

$$L = \int_S ((Wn_x - (p_x \varepsilon_{xx} + p_y \frac{\partial u_y}{\partial x}))y - (Wn_y - (p_x \frac{\partial u_y}{\partial x} + p_y \varepsilon_{yy}))x + p_x u_y + p_y u_x)dS \tag{8}$$

$$M = \int_S ((Wn_x - (p_x \varepsilon_{xx} + p_y \frac{\partial u_y}{\partial x}))x - (Wn_y - (p_x \frac{\partial u_y}{\partial x} + p_y \varepsilon_{yy}))y_x)dS \tag{9}$$

vanish for arbitrary closed integration paths S surrounding a homogeneous singly connected isotropic elastic domain. In Eqn. 6-9 W is the strain energy density, n_i is the unit outward normal vector of S, u_i is the deformation vector, ε_{ij} is the first order strain measure, p_i is the traction vector at S, corresponding to the unit outward normal vector and finally, x and y are coordinates of points at S. The subscripts refer to components in a global Cartesian reference frame (see Fig. (3)).

If a defect is present in the domain and the integration path S completely surrounds the defect, these integrals differ from zero and express energy changes in the domain corresponding to certain defect variations. Eshelby [4] has shown that the energy release rate for an infinitesimal translation δr can be determined by means of J_x and J_y, whereas Budiansky/Rice [5] have shown that the energy release rate for an infinitesimal rotation and an infinitesimal expansion can be determined by means of L and M. This may be summarized in the following formulae, which give the energy release rate associated with infinitesimal variations of defects:

| Translation | $\mathbf{r'} = \mathbf{r} + \boldsymbol{\delta r}$ | $\delta\Pi = \delta r_x J_x + \delta r_y J_y$ | (10) |

$$\text{Translation} \quad \mathbf{r'} = \mathbf{r} + \boldsymbol{\delta r} \qquad \delta\Pi = \delta r_x J_x + \delta r_y J_y \tag{10}$$

$$\text{Rotation} \quad \mathbf{r'} = \Omega\mathbf{r}, \left(\Omega = \delta\omega\begin{bmatrix} 0 & -1 \\ 1 & 1 \end{bmatrix}\right) \quad \delta\Pi = -\delta\omega L \tag{11}$$

$$\text{Expansion} \quad \mathbf{r'} = (1+\delta f)\mathbf{r} \qquad \delta\Pi = \delta f M \tag{12}$$
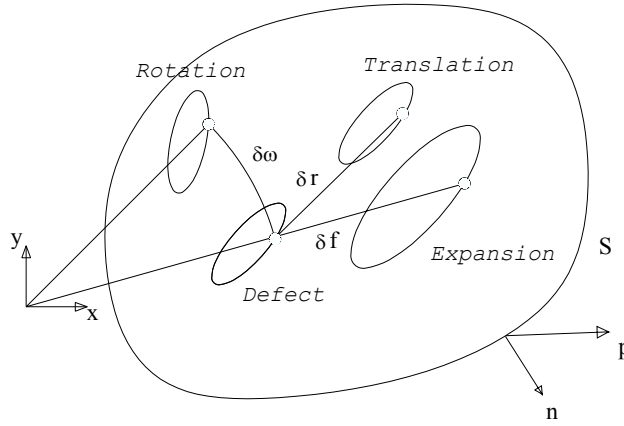

Figure 3 Various defect variations, translation, rotation and expansion, in an elastic domain.

PREDICTING THE DIRECTION OF CRACK PROPAGATION

Based on the energy release rates presented in the previous section, two proposals for predicting the direction of crack propagation are now made. The proposals are depicted in Fig.(4). The current crack tip is positioned such that the stresses are completely smooth. Firstly the crack tip is advanced a distance Δ in the tangential direction, a direction adhering to the $J_y=0$ or $L=0$ principles. For this predicted crack, the external load and the tractions in the process zone are determined, using the principle of superposition requiring the first principal stress to equal the tensile strength. Secondly, for this configuration the energy release rate with regard to the predicted crack is determined and the direction of crack propagation is derived from the virtual displacements of the predicted crack, as shown in Fig.(4). In proposal A the predicted crack is given virtual translations, whereas in proposal B the predicted crack is expanded and rotated. The energy release rate for the two proposals respectively is:

$$\delta\Pi = \begin{cases} J_x\delta r_x + J_y\delta r_y & \text{Proposal A} \\ \Delta(M\delta r_x - L\delta r_y) & \text{Proposal B} \end{cases} \tag{13}$$
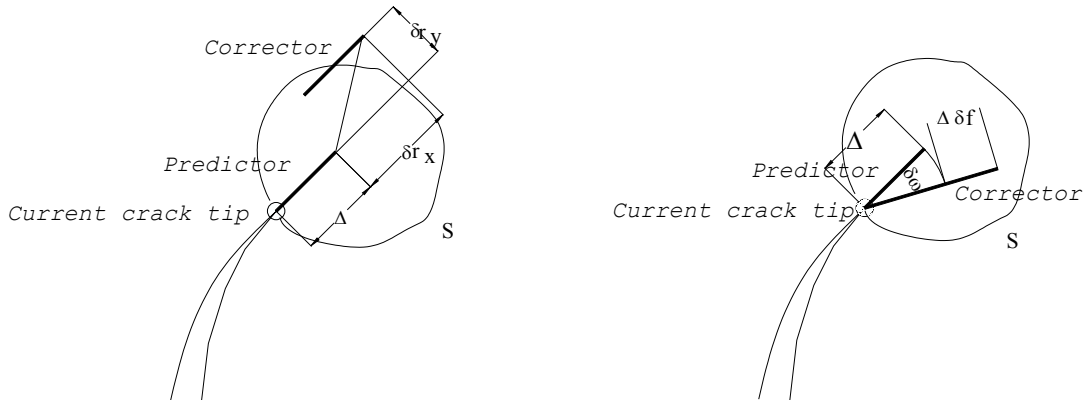

Figure 4 Proposals for predicting the direction of crack propagation.

From Eqn.(13), using the principle of maximum energy release rate, the direction of crack advance α is now determined from :

$$\alpha = Arctg \begin{cases} \dfrac{J_y}{J_x} & \textit{Proposal A} \\ -\dfrac{L}{M} & \textit{Proposal B} \end{cases} \qquad (14)$$

For the beam studied previously, the direction of crack propagation is plotted in Fig.(5) for various directions of the crack predictor. It was seen previously that the minimum energy configuration was achieved for a crack tip position corresponding to approximately $v=20^o$, with a rather flat functional variation within the interval $v=17^o$ to $v=22^o$. With proposal A the corrected direction of crack propagation is rather insensitive to the direction of the crack predictor and lies in the interval $v=15.8\text{-}17.3^o$, however, slightly below the expected direction of propagation. Proposal B is very sensitive to the direction of the crack predictor. However, within a range of $\pm 3^o$, the proper direction of crack propagation is determined fairly accurately.
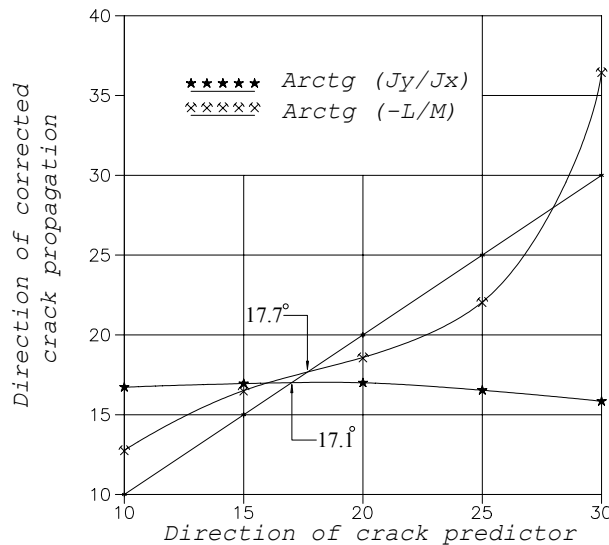

Figure 5 Prediction of the direction of crack propagation for various directions of the predictor.

CONCLUSION

In mixed mode fracture applying the fictitious crack model, the direction of crack propagation may be accurately predicted by evaluation of the *J, L* and *M* integrals. Directions based on $J_y=0$ and $L=0$ criteria are derived. These directions closely predict a path corresponding to minimum potential energy.

REFERENCES

1. Hillerborg, A, Peterson, P.E. : Analysis of crack formation and crack growth in concrete by means of fracture mechanics and finite elements. Cement and Concrete Research, 6:773-782,1976.
2. Peterson, P.E. : Crack growth and development of fracture zones in plain concrete and similar materials, TVBM-1006, thesis, Division of Building Materials, University of Lund, Sweden, 1981.
3. Ingraffea, A.R., Saouma, V. : Numerical Modeling of Discrete Crack Propagation in Reinforced and Plain Concrete, Fracture Mechanics of Concrete, Martinus Nijhoff Publishers, Dordrecht, pp.171-225, 1985
4. Eshelby, J.D. : Energy Relations and the Energy-Momentum Tensor in Continuum Mechanics, in Inelastic Behaviour of Solids, Ed. M.F. Kanninen et al, McGraw-Hill, New York, 1970, pp. 77-114.
5. Budiansky, B., Rice J.R. : Conservation Laws and Energy_Release Rates, J. Appl. Mech. No. 40, March 1973, pp. 201-203.
6. Brebbia, C.A., Telles J.C.F., Wrobel, L.C. : Boundary Element Techniques, Springer-Verlag, Berlin and New York, 1984.